

# Impact of Navier Slip and Wall Permeability in Unsteady of Nanofluid with Convective Cooling

Michael H. Mkwizu<sup>1</sup>

<sup>1</sup> Department of Mathematics and Statistics, College of Natural and Applied Sciences, Sokoine University of Agriculture, P.O.BOX, 3038, Morogoro-Tanzania

Received: 2 Jun. 2025, Revised: 30 July. 2025, Accepted: 25 Aug. 2025

Published online: 1 Sep. 2025

**Abstract:** The study aimed at conducting an investigation on effect of Navier slip and wall permeability in unsteady of nanofluid with convective cooling. Specifically the study intended to; develop flow model for a case of nanofluid in a channel, determine the effect of different parameters on velocity, temperature and to determine the effect of magnetic field. Findings showed that an increase of Reynolds number leads to increase in the velocity while pressure gradient, magnetic field and nanofluid fraction held constant. It is evidently that Alumina-water nanofluid tends to raise the velocity profile faster than Copper-water nanofluid. Furthermore the results show that an increase in Eckert number causes the decrease in temperature profile. It was noticed further that Copper-water nanofluid tends to raise the temperature profile faster than Alumina-water nanofluid.

Keywords: Navier slip, Wall permeability, Unsteady, Nanofluids.

### 1 Introduction

This study aimed to making an investigation on wall permeability in unsteady of nanofluid with convective cooling. Specifically the study intended to develop flow model for a case of nanofluid in a channel, determine the effect of different parameters on velocity and temperature on the wall permeability nanofluid channel flow. Nanofluids had large number of properties which was used in many applications. They are considered as superior than convectional fluids. Due to novel properties of nanofluids, it can be widely used for various heat transfer applications of engineering including brake fluids, automotive and air conditioning cooling, solar and power plant cooling, cooling of transformer oil, improving diesel generator efficiency, in nuclear reactor and defense and space as reported by Xiang and Arun [1].

Convectional fluids were suitable for heat transfer applications, but they had poor thermal conductivity as compared to nanofluids. Nanofluids can be considered to be the next-generation heat transfer performance compared to base liquids. Researchers have tried to increase the thermal conductivity of fluids by suspending micro sized particles in base fluids. Nanofluids are fluids in which nanoparticles of materials having high thermal conductivity such as metals, metal oxides, or carbon are suspended in to the base fluids. Nanofluids were known for their thermal conductivity, which may be quite enhanced as compared with that of just the base fluid or that of the bulk colloidal suspensions. This property is useful in extracting more energy from nuclear and geothermal power enhancing their efficiencies.

The Navier slip condition is derived as the effective boundary condition, in the limit as the roughness becomes small; it was the first order corrector to the no-slip condition on the limiting smooth surface. The slip length ,was simple measure of slip magnitude was apparently the most commonly used (material) parameter to characterize the slip .physically the slip length corresponds to the distance below the surface at which a linear extrapolation of the velocity profile would satisfy the non-slip boundary condition. Normally, when the slip length is very small compared to the dimensions of the flow path the effect of slip diminishes and could become negligible although this may not be true in general. A large slip length indicates that the liquid flow between confining surfaces experiences a lower friction and a solid moving in a liquid experiences a lower drag force.

<sup>\*</sup> Corresponding author e-mail: mkwizu@sua.ac.tz



Mkwizu, Makinde, Nkansah-Gyekye [2] did the study on Effects of Navier slip and wall permeability on entropy generation in unsteady generalized Couette flow of nanofluids with convective cooling. They found that an increase in nanoparticles volume fraction and Reynolds number causes a decrease in the velocity profile. Meanwhile nanofluid velocity profile increases with an increase in pressure gradient. The temperature profile increases with an increase in the nanoparticles volume fraction, slip parameter and Eckert number. But a decrease in temperature profile is noticed with an increase in Biot number. Skin friction increases with an increase in nanoparticles volume fraction slip parameter and Reynolds number. But decrease with an increase in pressure gradient. The same results are obtained for the Nusselt number. A rise in an entropy generation rate is observed with an increase in nanoparticles volume fraction and slip parameter. It falls near the lower wall and rises near the upper wall with an increase in Biot number. The Bejan number increase with time at the lower and upper walls but slight decreases at the channel centerline. It increases at the walls with an increase in nanoparticles volume fraction. As Biot number and pressure gradient increases, Bejan number decreases near the lower wall and at the center, but increases as it approaches the upper wall. Eckert number causes the increase in Bejan number at the lower and upper walls.

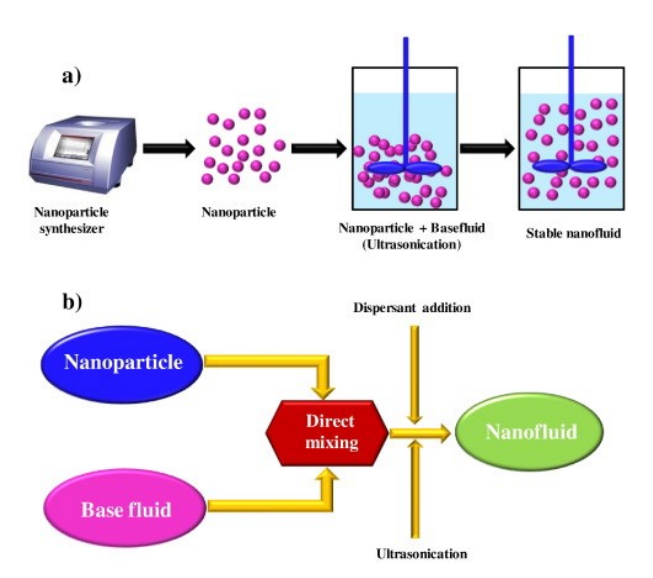


Fig. 1: Schematic representation of nanoparticle.

Shit G. C, Haldar, R and S. Mandal [3] did the study on the entropy generation on MHD flow and convective heat transfer in a porous medium of exponentially stretching surface saturated by nanofluids. The study shows that the thermal boundary layer thickness significantly increases with the increase of Brownian motion, thermophoresis number and magnetic field strength. The unsteadiness behavior of the flow of nanofluid has reducing effect on both momentum and thermal boundary layer thickness. The Brownian motion has controlling effect on nanoparticle migration. The entropy generation by means of Bejan number has strong impact on the applied magnetic field, dissipation of energy, thermal radiation and Biot number.

Makinde *et al.* [4] discussed the analysis of heat transfer in Berman flow of nanofluids with Navier slip, viscous dissipation, and convective cooling. Heat transfer characteristics of a Berman flow of water-based nanofluids containing copper (Cu) and alumina ( $Al_2O_3$ ) as nanoparticles in a porous channel with Navier slip, viscous dissipation, and convective cooling were investigated. It was assumed that the exchange of heat with the ambient surrounding takes place at the channel walls following Newton's law of cooling. It was revealed that Cu-water nanofluid moves faster with enhanced flow reversal at the walls as compared to  $Al_2O_3$ —water nanofluid. Furthermore, Cu-water produced higher temperature as compared to  $Al_2O_3$ —water. The nanofluid temperature increases with suction, but decreases with injection.

Dodda Ramya *et al.* [5] discussed the effect of velocity and thermal wall slip on magnetohydrodynamic (MHD) boundary layer viscous flow and heat transfer of a nanofluid over a non-linearly stretching sheet. It was found that as the



velocity slip parameter increased, the velocity profile decreased, and both the skin friction and heat transfer decreased, while the mass transfer rate increased.

Rundora and Makinde [6] studied the effects of Navier slip on unsteady flow of a reactive variable viscosity non-Newtonian fluid through a porous saturated medium with asymmetric convective boundary conditions. They found that the lower wall slip parameter was observed to increase the fluid velocity profiles, whereas the upper wall slip parameter retards. Heat production in the fluid was seen to increase with the slip parameters. The wall shear stress increases with the slip parameters while the wall heat transfer rate is largely unaltered by the lower wall slip parameter.

Wang and Mujumdar [7] presented a comprehensive review of heat transfer characteristics of nanofluids. Detailed reports on convective transport in nanofluids can be found in Buongiorno [8], and Tiwari and Das [9]. Mkwizu and Makinde [10] investigated entropy generation in a variable viscosity channel flow of nanofluids with convective cooling and found that, by careful combination of parameter values, the entropy production within the channel flow of a variable-viscosity water-based nanofluid in the presence of convective cooling can be minimized. These parameters are the Eckert number (Ec), Biot number (Bi), thermophoresis parameter (Nt), and so on.

Mfinanga [11] focused on numerical investigation of the effect of parameters in nanofluid flows in a channel with Navier slip and convective cooling. Results revealed that Alumina—water nanofluid tends to flow faster than Cu—water nanofluid. For both Alumina—water and Cu—water nanofluids, their velocity increases with time until they reach steady state, but Alumina—water reaches its steady state earlier than Cu—water. The nanofluid velocity increases with Reynolds number (Re) and pressure gradient (A), but decreases with an increase of nanoparticle volume fraction  $\phi$ . The nanofluid velocity is maximum at the lower plate of the channel flow and minimum at the wall of the upper plate as the space increases. The temperature of Alumina—water nanofluids rises faster than that of Cu—water nanofluids. The nanofluid temperature increases with Eckert number (Ec) and space, but a decrease in nanofluid temperature is noticed with an increase of Biot number (Bi) and nanoparticle volume fraction ( $\phi$ ).

Hydromagnetic blood flow through a uniform channel with permeable walls covered by porous media of finite thickness was studied by Ramakrishnan and Shailendhra [12]. They found that the axial velocity of the fluid is reduced by the porous parameter and the Hartmann number.

# 2 Mathematical model

Consider unsteady laminar flow of viscous incompressible nanofluids containing Copper (Cu) and Alumina (Al<sub>2</sub>O<sub>3</sub>) as nanoparticles through a channel with permeable walls. It is assumed that the fluid is injected uniformly into the channel at the lower plate, while uniform fluid suction occurs at the moving upper plate, as depicted in Figure 2.

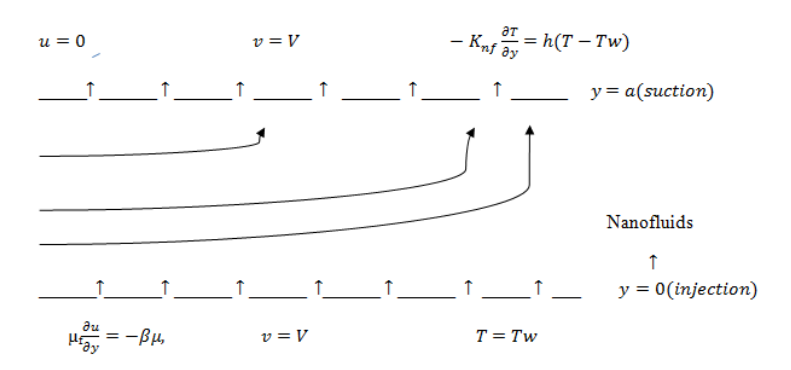


Fig. 2: Schematic diagram of the problem under consideration

The governing equations for nanofluid momentum and energy can be written as follows

$$\frac{\partial u}{\partial t} + V \frac{\partial u}{\partial y} = -\frac{1}{\rho_{nf}} \frac{\partial p}{\partial x} + \frac{\mu_{nf}}{\rho_{nf}} \frac{\partial^2 u}{\partial y^2},\tag{1}$$



$$\frac{\partial T}{\partial t} + V \frac{\partial T}{\partial y} = \alpha_{nf} \frac{\partial^2 T}{\partial y^2} + \frac{\alpha_{nf} \mu_{nf}}{K_{nf}} \left( \frac{\partial u}{\partial y} \right)^2. \tag{2}$$

Where u is the nanofluid velocity in the x-direction, T is the temperature of the nanofluid, p is the pressure, t is the time, a is the channel width,  $T_w$  is the lower stationary wall temperature,  $\mu_{nf}$  is the dynamic viscosity of the nanofluid,  $K_{nf}$  the nanofluid thermal conductivity,  $\rho_{nf}$  is the density of the nanofluid and  $\alpha_{nf}$  is the thermal diffusivity of the nanofluid which are given by

$$\mu_{nf} = \frac{\mu_f}{(1 - \varphi)^{2.5}}, \quad \rho_{nf} = (1 - \varphi)\rho_f + \varphi \rho_s,$$

$$\alpha_{nf} = \frac{K_{nf}}{(\rho c_p)_{nf}}, \quad \tau = \frac{(\rho c_p)_s}{(\rho c_p)_f} \frac{K_{nf}}{k_f} = \frac{(k_s - 2k_f) - 2\varphi(k_f - k_s)}{(k_s + 2k_f) + \varphi(k_f - k_s)},$$

$$(\rho c_p)_{nf} = (1 - \varphi)(\rho c_p)_f + \varphi(\rho c_p)_s.$$
(3)

The nanoparticles volume fraction was represented by  $\varphi$  ( $\varphi = 0$  corresponds to a base fluid),  $\rho_f$  and  $\rho_s$  are the densities of the base fluid and the nanoparticles respectively,  $k_f$  and  $k_s$  are the thermal conductivities of the base fluid and nanoparticles respectively,  $(\rho c_p)_f$  and  $(\rho c_p)_s$  are the heat capacities of the base fluid and the nanoparticles respectively.

It is worth mentioning that the use of the above expression for  $K_{nf}$  was restricted to spherical nanoparticles and does not account for other shapes of nanoparticles. Also, approximation has been employed to approximate the effective dynamic viscosity of the nanofluid  $\mu_{nf}$  as the viscosity of a base fluid  $\mu_f$  containing dilute suspension of fine spherical particles the initial and boundary condition are given as follows

$$u(y,0) = 0, \quad T(y,0) = T_W$$
 (4)

$$\mu_f \frac{\partial u}{\partial y} = -\beta u(0, t), \quad T(0, t) = T_W \tag{5}$$

$$u(h,t) = U, \quad -K_{nf} \frac{\partial u}{\partial v}(h,t) = h(T(a,t) - T_W). \tag{6}$$

Table 1: Thermal physical properties of nanoparticles and water

Physical properties	Fluid phase (water)	Copper (Cu)	Alumina (Al <sub>2</sub> O <sub>3</sub> )
$c_p$ (J/kg K)	4179	385	765
$\rho$ (kg/m <sup>3</sup> )	997.1	8933	3970
k (W/m K)	0.613	401	40

The following are non-dimensional variable and parameter quantities:

$$\theta = \frac{T - T_W}{T_W}, \quad W = \frac{u}{U}, \quad t = \frac{tV}{h}, \quad v_f = \frac{\mu_f}{\rho_f}, \quad \bar{P} = \frac{Ph}{\mu_f},$$

$$A = \frac{\partial \bar{P}}{\partial X}, \quad X = \frac{x}{a}, \quad \eta = \frac{y}{h},$$

$$Pr = \frac{\mu_f c_{pf}}{k_f}, \quad Ec = \frac{U^2}{c_{pf} T_a}, \quad \tau = \frac{(\rho c_p)_s}{(\rho c_p)_f},$$

$$m = \frac{(k_s + 2k_f) + \varphi(k_f - k_s)}{(k_s + 2k_f) - 2\varphi(k_f - k_s)}, \quad Re = \frac{Vh}{v_f}, \quad \alpha_f = \frac{k_f}{(\rho c_p)_f}, \quad f = \frac{\mu_f}{\beta h}.$$
(7)



Where *Pr* represents the Prandtl number, *Ec* stands for the Eckert number, *Re* is the Reynolds number, and *A* stands for the pressure gradient parameter. The dimensionless governing equations together with the appropriate initial and boundary conditions can be written as:

$$\frac{\partial W}{\partial t} = -\frac{A}{Re(1 - \varphi + \varphi \frac{\rho_s}{\rho_f})} + \frac{1}{Re(1 - \varphi + \varphi \frac{\rho_s}{\rho_f})(1 - \varphi)^{2.5}} \frac{\partial^2 W}{\partial \eta^2} - \frac{\partial W}{\partial \eta}$$
(8)

$$\frac{\partial \theta}{\partial t} = \frac{1}{mPrRe(1 - \varphi + \varphi \tau)} \frac{\partial^2 \theta}{\partial \eta^2} + \frac{Ec}{Re(1 - \varphi)^{2.5}(1 - \varphi + \varphi \tau)} \left(\frac{\partial W}{\partial \eta}\right)^2 - \frac{\partial \theta}{\partial \eta}$$
(9)

The initial and boundary conditions for equations (8) and (9) can be written as follows:

$$W(\eta, 0) = \theta(\eta, 0) = 0 \tag{10}$$

$$\frac{\partial W}{\partial \eta}(0,t) = -\frac{\beta a}{\mu_f} W(0,t), \quad \theta(0,t) = 0$$
(11)

$$W(1,t) = 1, \quad \frac{\partial \theta}{\partial \eta}(1,t) = -m\beta i\theta(1,t). \tag{12}$$

### 3 Numerical Procedure

By using a semi-discretization finite difference method, the nonlinear initial boundary value problem (IBVP) in equations (8)–(12) can be solved numerically. We partition the spatial interval into equal parts and define grid size and grid points. The first and second spatial derivatives in equations (8) and (9) are approximated with second-order central finite differences. Then the semi-discrete system for the problem becomes:

$$\frac{dW}{dt} = \frac{-A}{Re(1 - \varphi + \varphi \frac{\rho_s}{\rho_f})} + \frac{W_{i+1} - 2W_i + W_{i-1}}{Re(1 - \varphi + \varphi \frac{\rho_s}{\rho_f})(1 - \varphi)^{2.5}(\Delta \eta)^2} - \frac{W_{i+1} - W_{i-1}}{2\Delta \eta}$$
(13)

$$\frac{d\theta}{dt} = \frac{\theta_{i+1} - 2\theta_i + \theta_{i-1}}{mPrRe(1 - \varphi + \varphi\tau)(\Delta\eta)^2} + \frac{Ec}{Re(1 - \varphi + \varphi\tau)(1 - \varphi)^{2.5}} \left(\frac{W_{i+1} - W_{i-1}}{2\Delta\eta}\right)^2 - \frac{\theta_{i+1} - \theta_{i-1}}{2\Delta\eta}$$
(14)

with initial conditions and boundary conditions

$$W_i(0) = \theta_i(0) = 0, \quad 1 < i < N+1.$$

Equations (13) and (14) are first-order ordinary differential equations with known initial conditions. So they can be easily solved iteratively using Runge-Kutta Fehlberg integration technique implemented on computer using MATLAB.

#### 4 Results and Discussions

Numerical solution for the representative velocity field and temperature field has been carried out by assigning some arbitrary chosen specific values to various thermophysical parameters controlling the flow system. Following K.S. Hwang, J.-H. Lee, S.P. Jang [13], the Prandtl number (Pr) of the pure water-based nanofluid under consideration is assigned the value 6.2.



# 4.1 Effect of Parameter Variation on Velocity Profiles

The effects of parameter variation on velocity profiles are displayed in Figures 3–9 as follows: From Figure 3 it is noted that, the velocity increases with time for a given set of parameter values until a steady state profile is achieved. Also from this figure it is observed that alumina—water nanofluid tends to flow faster than copper—water nanofluids. This observation may be attributed to the difference in density between alumina—water nanofluid and copper—water nanofluids, due to the high density of copper nanoparticles as compared to alumina nanoparticles. Numerical investigation of the effects of convective cooling, Navier slip, and wall permeability in unsteady flow of water-based nanofluids containing Copper (Cu) and Alumina (Al<sub>2</sub>O<sub>3</sub>) nanoparticles has been presented. By applying a semi-discretization method together with the Runge-Kutta integration method, the problem was solved numerically. The following are the summary of the obtained results: An increase in nanoparticles and Reynolds number leads to increase in the velocity while pressure gradient and nanofluid fraction held constant. It is evidently that Alumina-water nanofluid tends to raise the velocity profile faster than Copper-water nanofluid. Also the results show that an increase in Eckert number causes the decrease in temperature profile. Further, it is noticed that Copper-water nanofluid tends to raise the temperature profile faster than Alumina-water nanofluid.

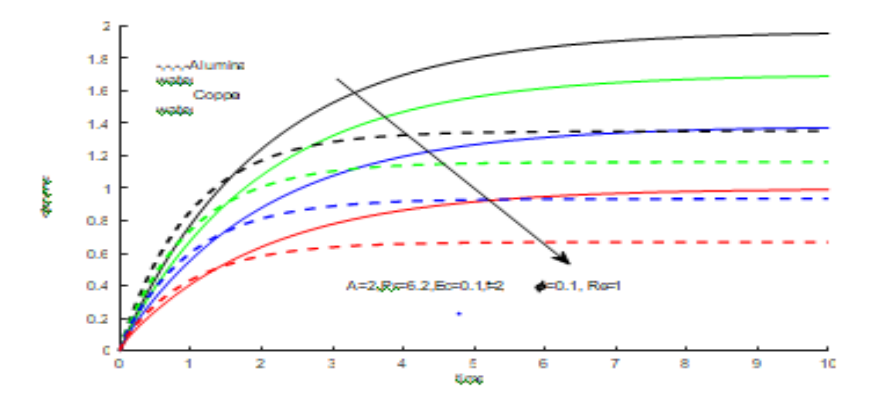


Fig. 3: Nanofluids velocity profile with increasing time

Looking to Figure 4, it can be noted that as space increases the velocity of nanofluid also increases. Also the observation shows that Alumina-water nanofluid tends to raise the velocity profile faster than copper-water due to the fact that copper has high density compared to Alumina. In a nutshell the nanoparticles bring effect at a very small space with a very small change in time.

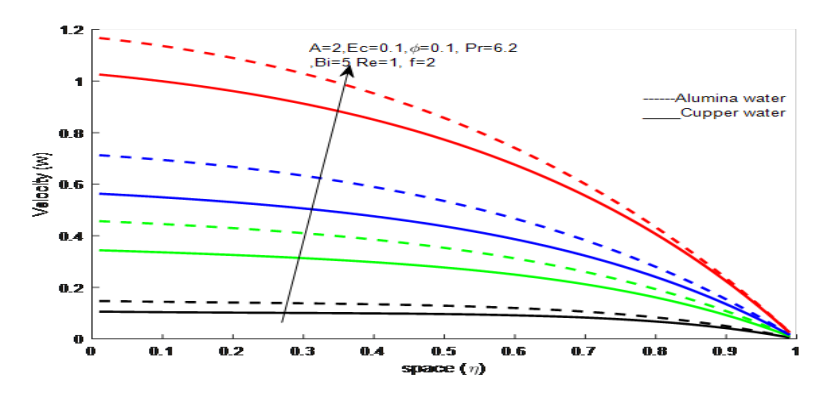
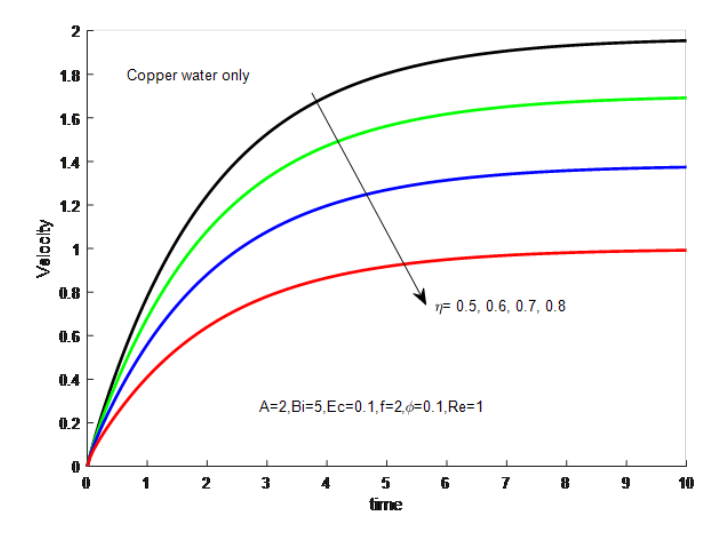


Fig. 4: Nanofluids velocity profile with increasing space

In figure 5 it can be not that an increase in time the nanofluid (copper water) velocity increase and with decrease in space the velocity of nanofluid increase.in real life situation when space increase the velocity of nanofluid decrease.



**Fig. 5:** Nanofluids velocity profile with increase space  $\eta$ 

In figure 6 show that the velocity decrease as space increase and when time increase also velocity increase when look on the graph above as see the time increase the velocity of nanofluid(copper water) also as space increase the velocity decrease may be due to particle in water, pressure and slip condition.

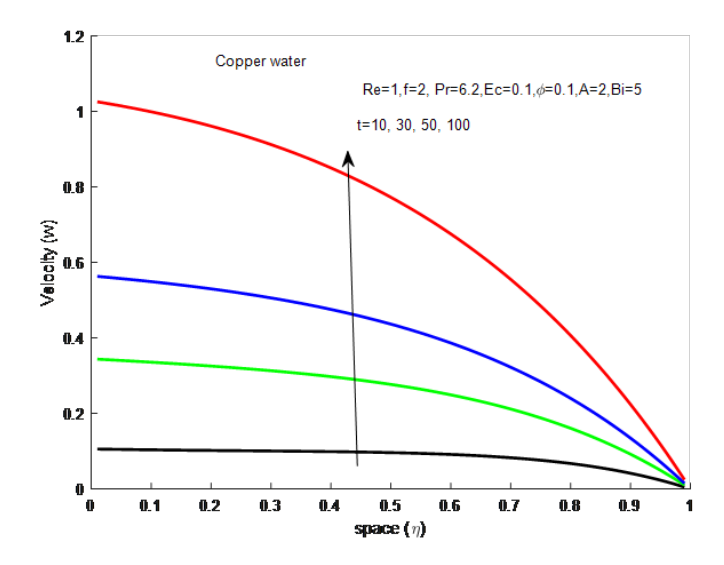
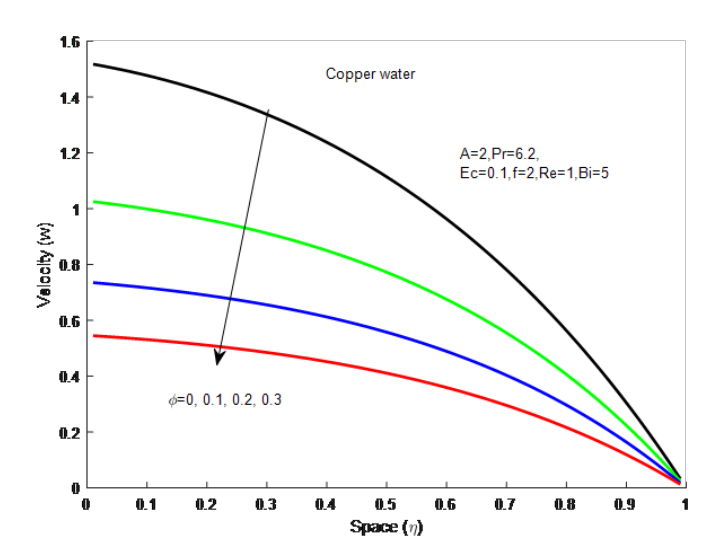


Fig. 6: Nanofluids velocity profile with increasing in t

From Figure 7, it is noted that an increase in nanoparticles volume fraction ( $\varphi$ ) causes a slight decrease in the velocity profile. This may be due to the density, the dynamic viscosity of the nanofluid, slip condition, and suction and injection of the fluid.



**Fig. 7:** Nanofluid velocity profile with increasing with increasing  $\varphi$ 

In figure 8 where increasing Reynolds number cause a decrease in velocity profile. This happen because the viscous increasing within the flow system as we can see that when the Reynolds number is small the velocity of nanofluid (copper water) is higher this shown that Reynolds have great effect in nanofluid. The velocity of water decrease when nanofluids space increased in normal life situation when the space is large the velocity of water decrease this due to pressure constant, slip condition.

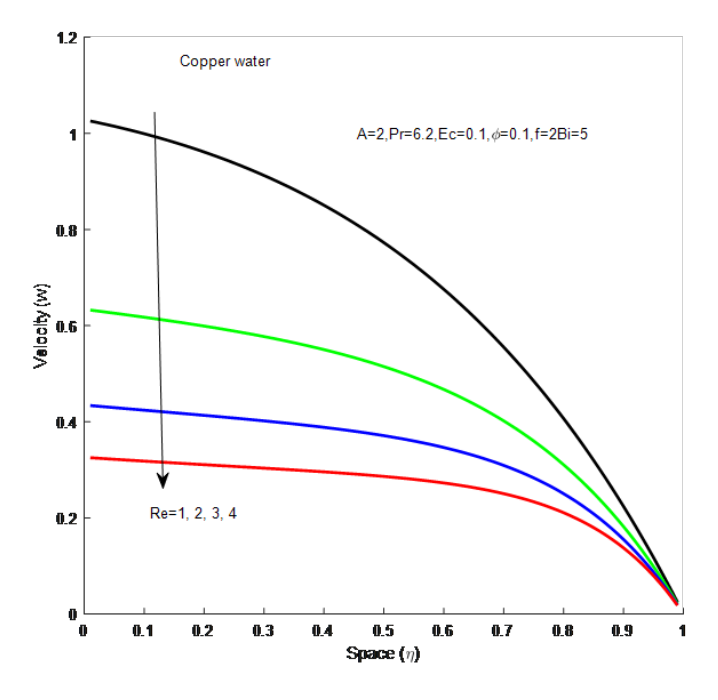


Fig. 8: Nanofluid velocity profile with increasing with increasing Re



Figure 9, shows that the nanofluid (cupper-water) particles velocity decreases with increase in space. Also in figure 7, it has been seen that the increase a pressure gradient (A) tends to raise the velocity of the profile. In other words the observation reveals that the higher the pressure gradient the significant the velocity profile. That is to say that of velocity increases with an increase in pressure gradient (A).

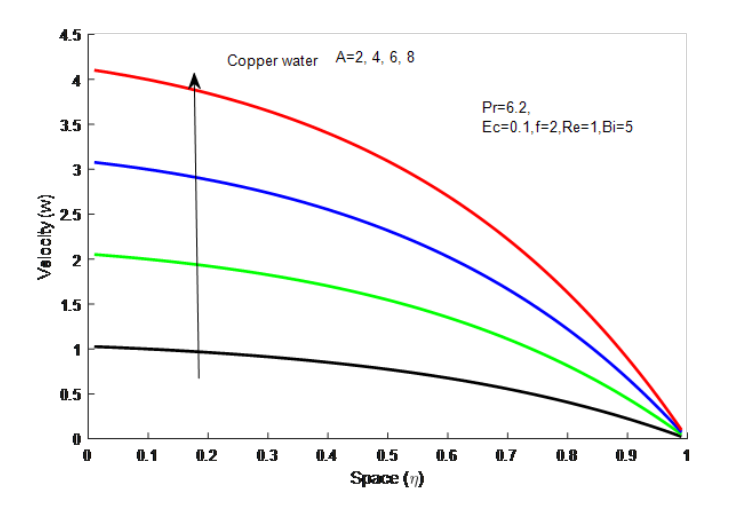


Fig. 9: Nanofluid velocity profiles with increasing A

# 4.2 Effects of Parameter Variation on Temperature Profiles

Figures 10–15 demonstrate the nanofluids temperature profiles across the channel and the effect of different parameters in the fluid flow system. Generally, due to convective heat loss to the ambient surroundings following Newton's law of cooling, the nanofluid temperature near the channel wall is decreasing.

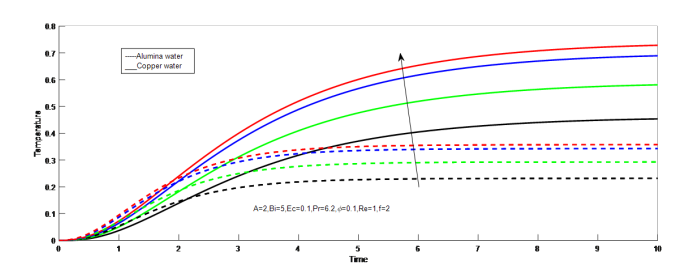


Fig. 10: Nanofluids temperature profiles with increasing time

From Figure 10 it is noted that the temperature increases with time near the lower wall it then increases toward the upper moving wall for a given set of parameter values until a corresponding steady state profile is achieved. This behavior may be attributed to the slip condition and injection at the lower wall, suction, and moving upper wall. Interestingly, the temperature of Cu-water nanofluid rises higher than that of Al<sub>2</sub>O<sub>3</sub>-water nanofluids.



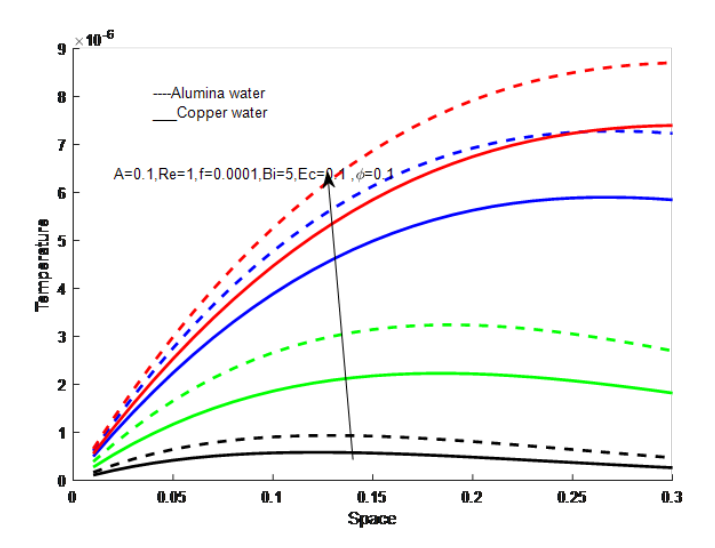
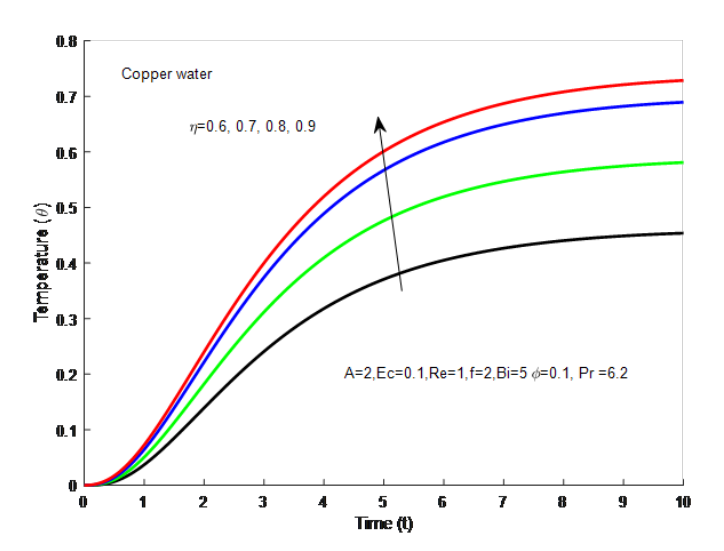


Fig. 11: Nanofluids temperature profiles with increasing space

Observing figure 11, it describes the results of temperature variation profiles with combined nanofluids Alumina-water and Copper-water. The result shows that the temperature increases with the increase in space. Also the observation shows that Alumina-water nanofluid tends to raise the temperature profile very fast than Copper-water nanofluid from a space this may be due to their differences in specific heat capacity and density



**Fig. 12:** Nanofluid temperature profile with increasing in  $\eta$ 

Figure 12 show that as time increase temperature of nanofluid (copper water) increase and space increase as temperature increases when look on the graph when time change increase the temperature of nanofluids also increase when the space of nanofluid (copper water) increase the temperature of water increase in real life situation when you have a large space the depth of nanofluid decrease hence its easily to be warmly or to hearted rather than the one with great depth.



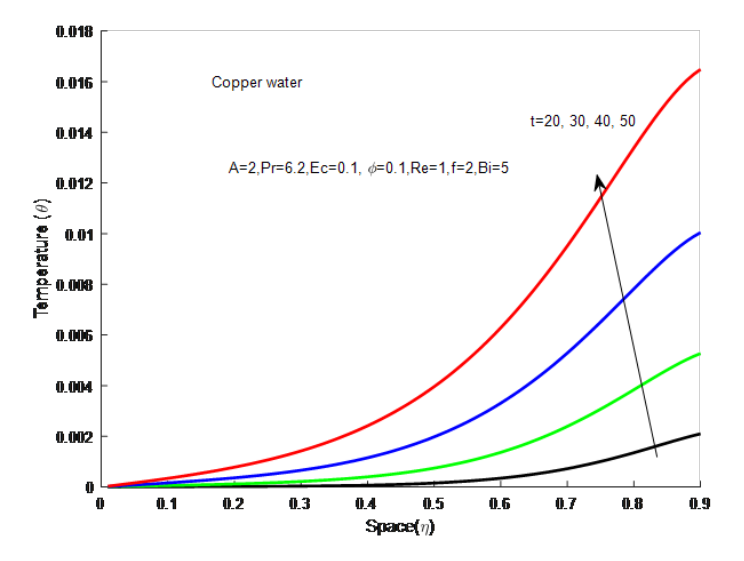


**Fig. 13:** Nanofluid temperature profile with increasing in  $\eta$ 

Figure 13 revealed that, the temperature increases with an increase in space. It can be noticed further that the temperature increases with an increase of time.

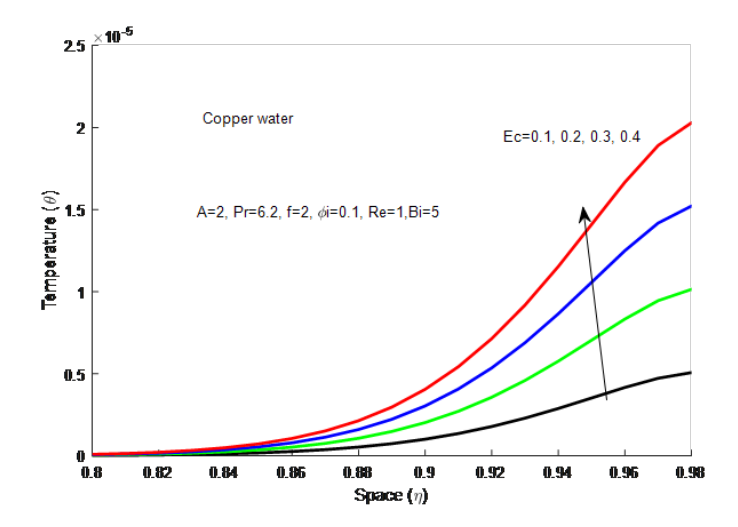


Fig. 14: Nanofluid temperature profile with increasing Ec

Figure 14 shows that with an increase in Eckert number the temperature profile also increases. This increase in temperature may be attributed by boundary of the flow (viscous dissipation) and the nature of the channel flow. For example in this observation it is noticed that at the lower plate of channel there no variation in temperature even Eckert number vary but at the upper plate of the channel there is a large increase in temperature in respond to the increase of Eckert number this may be due the relationship between the flows' kinetic energy and the boundary layer of the channel



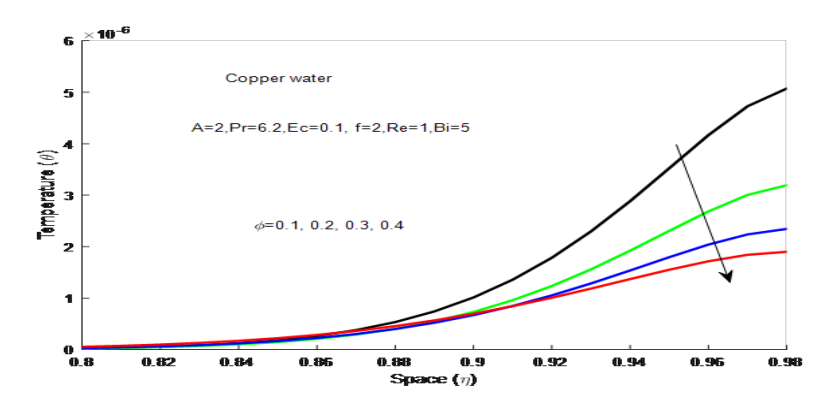


Fig. 15: Nanofluid temperature profile with increasing Ec

Figure 15 shows the temperature decreases with an increase of nanoparticle fraction  $(\phi)$ . This expected because nanoparticles as good conductor of heat, tends to absolve heat from the system which lead to cooling process to take place.

# **5 Conclusion**

A numerical investigation of the effects of convective cooling, Navier slip, and wall permeability in the unsteady flow of a channel containing water-based nanofluids with Copper (Cu) and Alumina (Al<sub>2</sub>O<sub>3</sub>) nanoparticles is presented. The governing problem is solved numerically using a semi-discretization method combined with the Runge-Kutta integration technique. The following summarizes the main results obtained: An increase in the nanoparticle volume fraction and Reynolds number leads to an increase in the velocity profile, while the pressure gradient and nanofluid fraction are held constant. It is observed that Alumina-water nanofluid increases the velocity profile faster than Copper-water nanofluid under the same conditions. The results show that an increase in the Eckert number causes a decrease in the temperature profile. Furthermore, Copper-water nanofluid tends to increase the temperature profile faster than Alumina-water nanofluid. These findings highlight the distinct effects of nanoparticle type and thermophysical parameters on the flow and heat transfer characteristics of water-based nanofluids in channel flows.

# **Nomenclature**

Main		Symbols
Symbol	Description	
и	Nanofluid velocity in the <i>x</i> -direction, m/s	
T	Temperature of the nanofluid, K	
P	Nanofluid pressure, Pa	
t	Time, s	
a	Channel width	
$T_w$	Lower stationary wall temperature	
$C_f$	Skin friction coefficient	
SG	Entropy generation rate	
NHTI	Heat transfer irreversibility	
NFFI	Fluid friction irreversibility	
Nu	Nusselt number	
Be	Bejan number	
Pr	Prandtl number	
Re	Reynolds number	
Ec	Eckert number	
Bi	Biot number	



Greek		Symbols
Symbol	Description	
$\mu_{nf}$	Dynamic viscosity of the nanofluid	
$k_{nf}$	Nanofluid thermal conductivity	
$ ho_{nf}$	Density of the nanofluid	
$\alpha_{nf}$	Thermal diffusivity of the nanofluid	
$\varphi$	Nanoparticles volume fraction	
$ ho_f$	Density of the base fluid, kg/m <sup>3</sup>	
$\rho_s$	Density of the nanoparticle, kg/m <sup>3</sup>	
$k_f$	Thermal conductivity of the base fluid	
$k_f \ k_s$	Thermal conductivity of the nanoparticles	
$(\rho c_p)_f$	Heat capacitance of the base fluid	
$(\rho c_p)_s$	Heat capacitance of the nanoparticles	

#### **Subscripts**

Symbol	Description	
f $nf$ $s$	Base fluid Nanofluid Nanoparticle	

## References

- [1] X.-Q. Wang and A. S. Mujumdar, A review on nanofluids-part I: theoretical and numerical investigations, *Brazilian Journal of Chemical Engineering*, vol. 25, pp. 613–630, 2008.
- [2] M. H. Mkwizu, O. D. Makinde, and Y. Nkansah-Gyekye, Effects of Navier slip and wall permeability on entropy generation in unsteady generalized Couette flow of nanofluids with convective cooling, *UPB Scientific Bulletin*, vol. 77, no. 4, pp. 201–216, 2015.
- [3] G. C. Shit, R. Haldar, and S. Mandal, Entropy generation on MHD flow and convective heat transfer in a porous medium of exponentially stretching surface saturated by nanofluids, *Advanced Powder Technology*, vol. 28, no. 6, pp. 1519–1530, 2017.
- [4] O. D. Makinde, S. Khamis, M. S. Tshehla, and O. Franks, Analysis of heat transfer in Berman flow of nanofluids with Navier slip, viscous dissipation, and convective cooling, *Advances in Mathematical Physics*, vol. 2014, no. 1, Art. ID 809367, 2014.
- [5] D. Ramya, R. Srinivasa Raju, J. Anand Rao, and A.J. Chamkha, Propulsion and Power Research 7(2), 182–195 (2018).
- [6] L. Rundora and O.D. Makinde, Journal of Hydrodynamics 27(6), 934–944 (2015).
- [7] X.-Q. Wang and A.S. Mujumdar, International Journal of Thermal Sciences 46(1), 1–19 (2007).
- [8] J. Buongiorno, Journal of Heat Transfer 128(3), 240-250 (2006).
- [9] R.K. Tiwari and M.K. Das, International Journal of Heat and Mass Transfer 50(9-10), 2002-2018 (2007).
- [10] M.H. Mkwizu and O.D. Makinde, Comptes Rendus Mécanique 343(1), 38-56 (2015).
- [11] I.S. Mfinanga, Numerical Investigation of the Effect of Parameters in Nanofluid Flows in a Channel with Navier Slip and Convective Cooling.
- [12] K. Ramakrishnan and K. Shailendhra, Journal of Applied Fluid Mechanics (JAFM) (2013).
- [13] K.S. Hwang, J.-H. Lee, and S.P. Jang, International Journal of Heat and Mass Transfer 50(19–20), 4003–4010 (2007).